Published in "Journal of Physics B: Atomic, Molecular and Optical Physics
44(6): 065201 , 2011" which should be cited to refer to this work.

Electron impact excitation of the ($4p^5$ 5s) states in krypton: high-resolution electron scattering experiments and B-spline R-matrix calculations

M Allan[1], O Zatsarinny[2] and K Bartschat[2]

[1] Department of Chemistry, University of Fribourg, 1700 Fribourg, Switzerland
[2] Department of Physics and Astronomy, Drake University, Des Moines, IA 50311, USA

E-mail: Michael.Allan@unifr.ch, oleg_zoi@yahoo.com and klaus.bartschat@drake.edu

Abstract
In a joint experimental and theoretical effort, we carried out a detailed study of electron impact excitation of the $4p^5$ 5s states of Kr. We present angle-differential cross sections over the entire angular range (0°–180°) for a number of energies in the near-threshold region, as well as energy scans for selected angles. The experimental results are in very satisfactory agreement with predictions from a fully relativistic Dirac B-spline R-matrix model.

1. Introduction

Electron impact excitation of the noble gases is an important problem in the field of electron–atom collisions. Numerous experimental and theoretical studies have been performed over many decades, both for fundamental as well as practical reasons. To name just one example in each area, the detailed study of the many near-threshold resonance features [1] has proven to be very challenging to both experiment and theory alike. The present study of partial differential cross sections (DCSs) represents an even more stringent test of theory than elastic or total metastable cross sections, because it also reveals the branching ratios for the decay of these resonances. On the practical side, a reliable knowledge of absolute inelastic cross sections for these processes is very important for applications in plasma and discharge physics, for example as used for lighting.

In a recent paper [2], we reported the results of a joint experimental and theoretical study of electron scattering from Kr atoms in the energy range of the low-lying $Kr^-(4p^5\,5s^2)$ Feshbach resonances. While very satisfactory agreement between the experimental data and results from semi-relativistic (Breit–Pauli) B-spline R-matrix (BSR) close-coupling calculations was achieved for the resonance features, particularly in elastic scattering, only qualitative agreement was obtained between the theoretical predictions and early experimental data of Phillips [3] for excitation of the four states in the ($4p^5$ 5s) manifold. Noteworthy discrepancies of up to about a factor of 2 occurred regarding the absolute scale of the angle-differential cross sections.

Given the importance of the problem, we decided to carry out further studies. Experimentally, it has become possible to scan the entire angular region 0°–180°, with an energy resolution of better than 15 meV. Theoretically, the semi-relativistic BSR method [4, 5] and a recently developed fully relativistic Dirac (DBSR) version [6] have achieved a breakthrough in the description of the near-threshold resonance features. Given that relativistic effects may need to be described beyond the Breit–Pauli approximation, and that even more states may need to be included in the close-coupling expansion, we decided to apply the DBSR approach to the problem at hand.

This paper is organized as follows. In section 2, we briefly describe the apparatus that was used to carry out the measurements. Section 3 then summarizes the numerical method employed in the calculations, with particular emphasis on the 69-state DBSR model. In section 4, we present the experimental results and compare them with previous measurements [3] and the (D)BSR predictions. We conclude with a brief summary.

2. Experiment

Electrons emitted from a hot filament were energy selected by a double hemispherical monochromator and focused onto an effusive beam target, introduced by a 0.25 mm nozzle kept at about 30°C. A double hemispherical analyser for detection of elastically or inelastically scattered electrons ensured background-free signals [7]. Absolute cross sections were determined by comparison against He using a relative-flow method [8]. A specially designed magnetic angle changer allowed for measurements up to 180° scattering angle [9]. The angular resolution is a convolution of the angular spread in the incident beam and the acceptance angle of the analyser. The combined resolution is about ±1.5° at 10 eV, with an estimated uncertainty in the angular position of ±2°. The angular acceptance increases with decreasing energy approximately as $E^{-1/2}$, for both the incident beam and the analyser acceptance cone. This is not critical in this work (in contrast to elastic scattering) because there are no sharp features in the angular distributions (except for the narrow forward peaks for dipole-allowed transitions). Procedures for ensuring reliable cross sections were described in detail elsewhere [10, 11]. The confidence limit (two standard deviations) for the absolute inelastic cross sections is about ±20%, but degrades to about ±25% at energies below 0.5 eV (measured respective to threshold for each process). The cross sections are only qualitative within the first 0.2 eV above threshold because drifts make the precise alignment of the incident beam and the analyser acceptance cone difficult. This problem is particularly severe at 0° and 180°, where only a small misalignment results in a large loss of signal. The present experimental cross sections are therefore likely too low within the first 0.2 eV above threshold for these two angles. The incident electron resolution was about 13 meV at a beam current of about 400 pA.

3. Theory

In our recent work, we employed a 47-state semi-relativistic BSR47 model, which was described in detail in [2] and hence will only be summarized briefly here. The core–valence correlation, inner-core correlation, the strong term dependence of the valence orbitals, and the very strong configuration mixing between the $4p^4\,(n+1)s$ and $4p^4\,nd$ states were all treated fully *ab initio*.

An important aspect of our approach is the use of *non-orthogonal*, *term-dependent* sets of radial functions for each individual state, also accounting for term mixing due to the spin–orbit interaction. In the BSR47 calculations, the atomic Hamiltonian included all one-electron Breit–Pauli operators plus the two-electron spin-other-orbit interaction. The relativistic corrections are very important in Kr, which is actually too heavy to expect excellent *ab initio* results in a perturbative approach with non-relativistic orbitals. Consequently, in order to reproduce the correct term mixing we used the experimental value of $\zeta(4p) = 0.666$ eV as the spin–orbit parameter for the 4p orbital. In contrast, the non-relativistic wavefunction for the $4s^2\,4p^5$ core yields $\zeta(4p) = 0.602$ eV, thus requiring a 10% adjustment.

The DBSR69 model used for this work is an extension of the DBSR31p model that was also described in detail in [2]. However, instead of the polarized pseudostate that was included in the model to represent the ground-state polarizability for elastic scattering, we added additional physical states in the expectation of better describing the resonance structure in the vicinity of the lowest few excitation thresholds. Specifically, we included all the states of principal configurations $4p^6$, $4p^5\,5s$, $4p^5\,5p$, $4p^5\,4d$, and $4p^5\,6s$ from the 31-state model, plus an additional 38 states built from the configurations $4p^5\,7s$, $4p^5\,6p$, $4p^5\,4d$, and $4p^5\,4f$, respectively. As before, the additional valence spinors were generated through a *B*-spline bound-state close-coupling calculation using a number of Kr^+ states with frozen core orbitals. The latter also included states with only one electron in the 4s orbital, and hence the model included the most important core–valence correlations in an *ab initio* manner.

We used the published BSR code [5] and our newly developed DBSR program [6] to solve the $(N+1)$-electron collision problem. The essential idea is to expand the basis of continuum orbitals used to describe the projectile electron inside the *R*-matrix box, i.e. the region where the problem is most complicated due to the highly correlated motion of $N+1$ electrons, also in terms of a *B*-spline basis. A semi-exponential grid for the *B*-spline knot sequence was set up to cover the inner region up to the *R*-matrix radius a. We used the same grid for the structure and the collision calculations. Even with the increased range of the additional states, the *R*-matrix box of $a = 50\,a_0$ (where $a_0 = 0.529 \times 10^{-10}$ m is the Bohr radius) was sufficient. We employed 111 *B*-splines to span this radial range. A dense mesh of knots near the origin was necessary in order to incorporate a finite-size nuclear model with a Fermi potential.

Note that the DBSR calculations lead to significantly larger interaction matrices in the internal region compared to the BSR calculations, due to the additional treatment of the small spinor components. In the DBSR69 calculations, which included up to 313 scattering channels, interaction matrices with dimensions of about 80 000 needed to be diagonalized. In order to perform those calculations we had to parallelize the DBSR code and also used parallelized linear-algebra libraries such as `SCALAPACK`.

We calculated partial-wave contributions up to $J = 51/2$ numerically. With such a high value of J, no extrapolation scheme to account for contributions from even higher partial waves was necessary for all observables presented in this paper. The cross sections of interest were then calculated in the same way as in the standard *R*-matrix approach. We employed an updated version [12] of the flexible asymptotic *R*-matrix (`FARM`) package by Burke and Noble [13] to solve the problem in the asymptotic region and to obtain the transition matrix elements of interest. After transforming the latter from the present jj-coupling to the jlK-coupling scheme and also accounting for the appropriate phase convention of the reduced matrix elements, we employed the program `MJK` of Grum-Grzhimailo [14] to calculate the angle-DCSs shown below.

4. Results and discussion

As mentioned above, comparison of our earlier predictions [2] with the experimental data of Phillips [3] revealed problems with the magnitude of the cross-sectional values. However, since these problems could be related to the angular dependence of the cross sections, a comparison at the nominal scattering angle without accounting for the angular resolution in the experiment might have been misleading. In the two subsections below we exhibit our present results, once as a function of energy for fixed scattering angles of 0°, 30°, 45°, 90°, 135°, 160°, and 180°, respectively, and once as a function of the scattering angle for fixed energies of 11.8, 13.0, 14.0, and 15.0 eV.

4.1. Energy scans at fixed scattering angle

Figures 1 and 2 exhibit the DCS as a function of energy for seven fixed scattering angles. Overall, we judge the agreement between the present measurements and the DBSR69 predictions as very satisfactory. Since the BSR47 results would be hard to distinguish from the DBSR69 curves in the graphs, we do not show them here. Although one might have suspected it, the good agreement between the DBSR69 and BSR47 results (one explicit comparison is given in the next subsection) confirms the consistency of our approach in two independently developed computer programs, and it gives us confidence that both relativistic effects and channel coupling have been treated to high accuracy in this work.

While the agreement between experiment and theory is certainly not perfect, the magnitude problems noted earlier in comparison with the data of Phillips [3] (see the panels for 30° and 90° in figure 1) are essentially resolved. We emphasize again that the present experimental data were normalized *independently* of the present theory by cross-normalization to the well-known elastic DCS for e–He collisions.

The largest remaining discrepancies between experiment and the DBSR69 predictions occur very close to threshold, in particular at the extreme angle of 180° (see figure 2). This problem is almost certainly related to drifts of the detector response function very close to threshold as explained in the experimental section—the detector did not 'see' the very low-energy electrons after the excitation process.

The other difference worth mentioning is that the theoretical results are lower than the experiment in the 12–14 eV energy range, in particular at 160° and 180°. Interestingly, the discrepancy occurs only for the $5s'[1/2]_1$ and $5s[3/2]_1$ states. This difference is very unlikely due to instrumental problems. Even if drifts caused imprecision of the instrumental response function (for which all spectra were corrected), such a problem would necessarily apply to all final states at a given scattering angle, since the spectra were recorded in an 'interleaved' manner. This means that the spectra for the four final states were recorded in succession, each for typically 30 min, with the cycle being repeated 3–25 times. This entire process was repeated 2–5 times at each scattering angle, with re-calibration of the response function on helium each time, to ensure reliability. In this way, even if a slow drift of the response function had occurred, it would have affected the results for all four final states at a given scattering angle to nearly the same degree. The total data acquisition time for each of the curves in figures 1 and 2 was typically 15 h.

4.2. Angle scans at fixed energy

Figure 3 exhibits the corresponding results as a function of the scattering angle for fixed incident projectile energies of 11.8, 13.0, 14.0, and 15.0 eV, respectively. Note that there is some overlap between figures 1 and 2 and figure 3. In principle, the cross section for a given state, angle, and energy should be the same in both the energy and angular scans. For the theoretical predictions, this is automatically the case. For the experimental data, on the other hand, it is not automatic since the drifts are different in the two scans. The good agreement between between the corresponding experimental data in the three figures is thus a critical test of the reliability of the experiment.

Once again, the overall agreement between theory and experiment is very satisfactory, with all major structures being reproduced by the DBSR69 model. At a first glance, the agreement may appear better in the energy scans than in the angular scan. A closer inspection, however, reveals that for the angles and energies that appear both in figures 1 and 2 and figure 3, the agreement is, apart from some experimental scatter, the same.

The only noticeable difference is that the calculated cross sections are below experiment at 180° for 13 and 14 eV, but only for the $5s'[1/2]_1$ and $5s[3/2]_1$ states. This difference has already been discussed in the preceding section in connection with the energy scans. Note that the $5s'[1/2]_1$ and $5s[3/2]_1$ states have narrow forward peaks at 13 and 14 eV, as expected for dipole-allowed transitions.

For the highest energy of 15 eV, we did not perform an angular scan, but we plot our DCS data for the seven angles at which we ran energy scans together with earlier experimental data of Trajmar *et al* [15] and of Guo *et al* [16]. Given the good agreement of our measurements with those of Trajmar *et al* [15] and both the DBSR69 and BSR47 predictions, we suspected a normalization error in the data published by Guo *et al* [16]. Indeed, this error was confirmed, and the published latter data should be multiplied by a factor of 0.37 [17]. This was done in the bottom right panel of figure 3.

As mentioned above, the comparison of the 15 eV BSR47 and DBSR69 results show very good agreement. In terms of the physical effects accounted for, this gives us confidence in the proper treatment of both relativistic effects and channel coupling. In addition, it reassures us of the numerical accuracy of our computer programs. Small differences between the two sets of predictions primarily occur near the backward direction, where the theoretical description seems to become more sensitive to the details of the computational model. This sensitivity is likely the reason for the remaining discrepancies between theory and experiment discussed in the previous subsection. It clearly emphasizes the usefulness of having experimental data available for comparison over the *entire* angular range, but particularly at 180°.

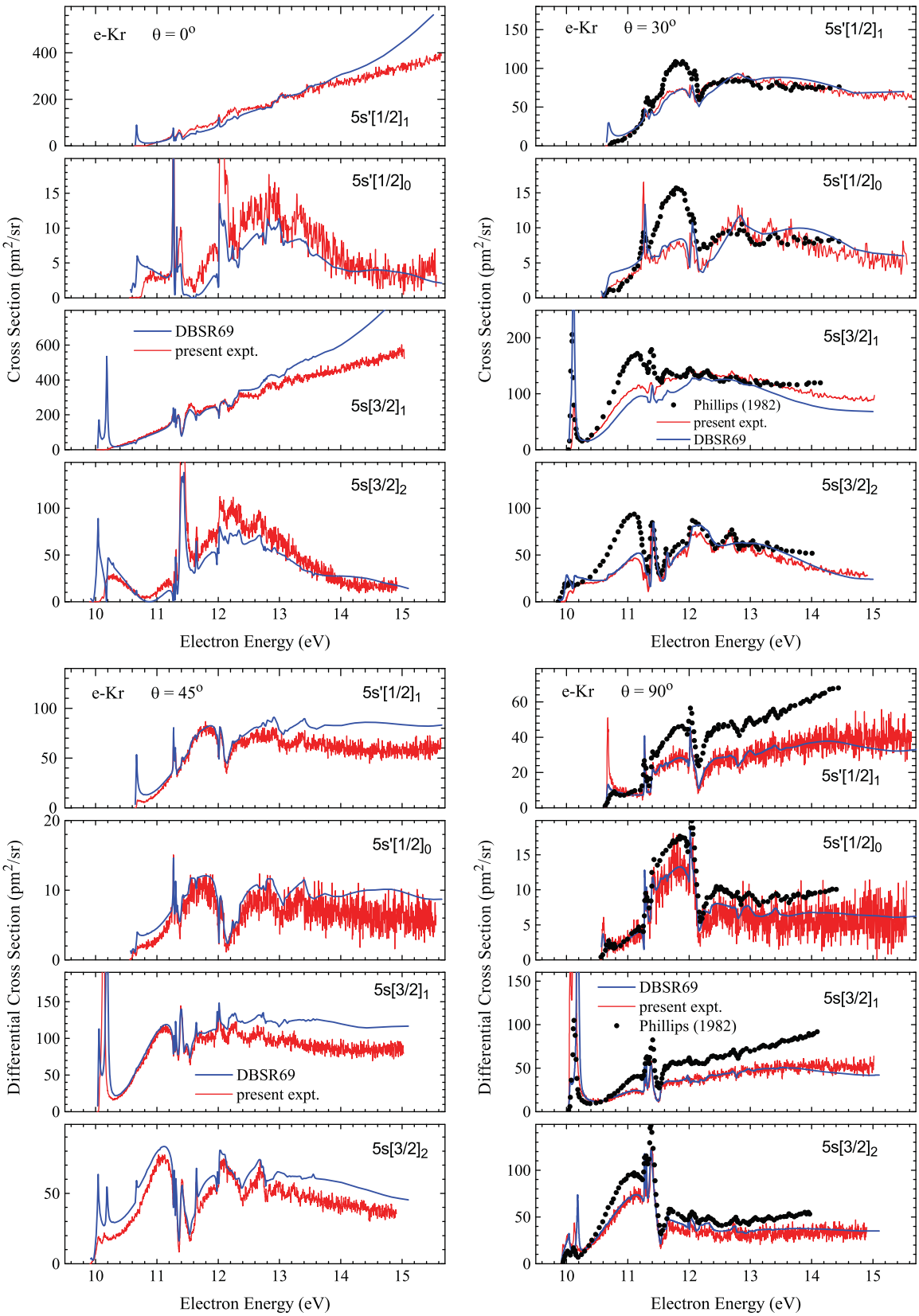

Figure 1. DCS for electron-impact excitation of Kr at scattering angles of 0°, 30°, 45°, and 90°. The experimental data are compared with theoretical predictions from the DBSR69 model. For 30° and 90°, we also show the experimental data of Phillips [3].

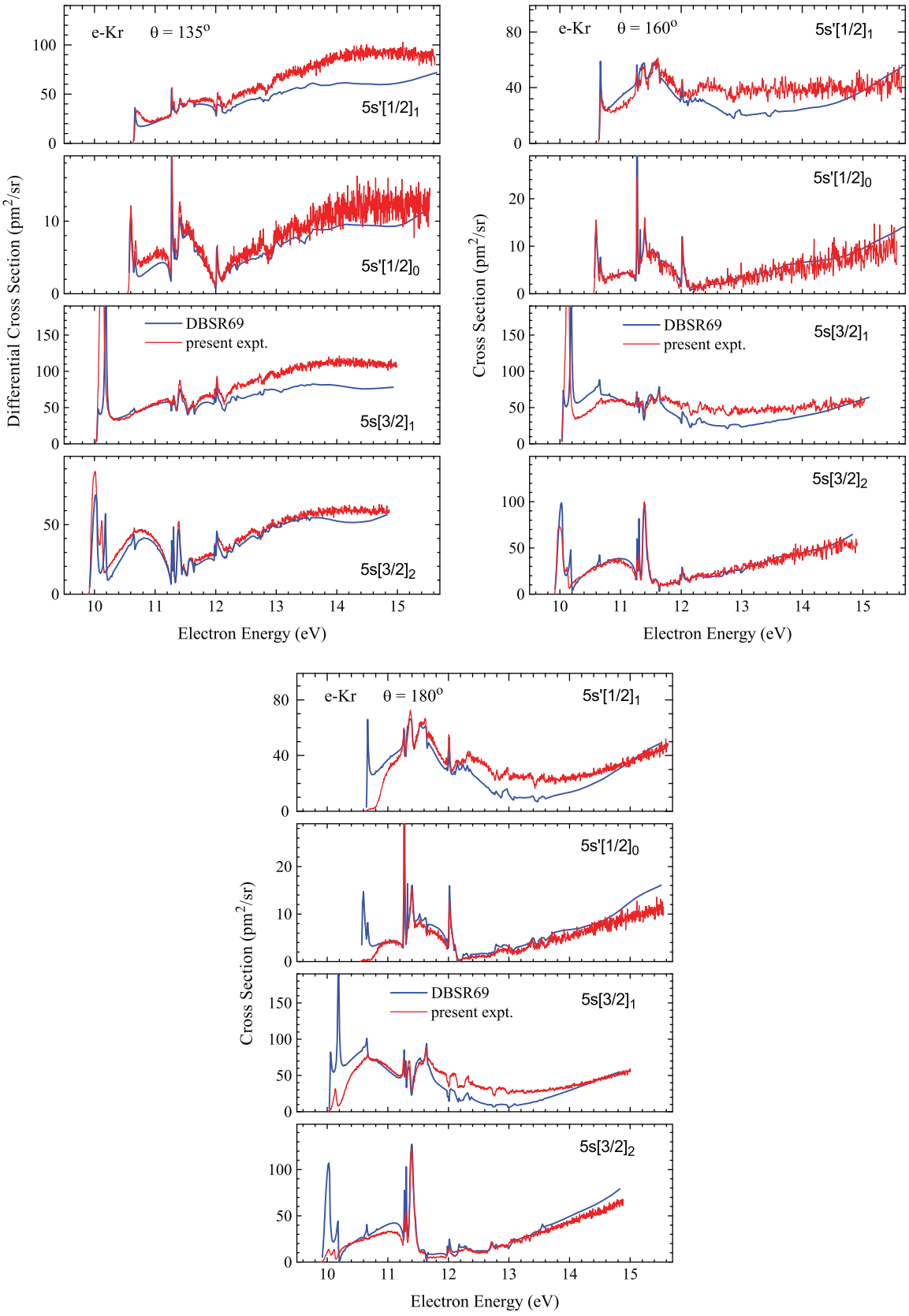

Figure 2. DCS for electron-impact excitation of Kr at scattering angles of 135°, 160°, and 180°. The experimental data are compared with theoretical predictions from the DBSR69 model.

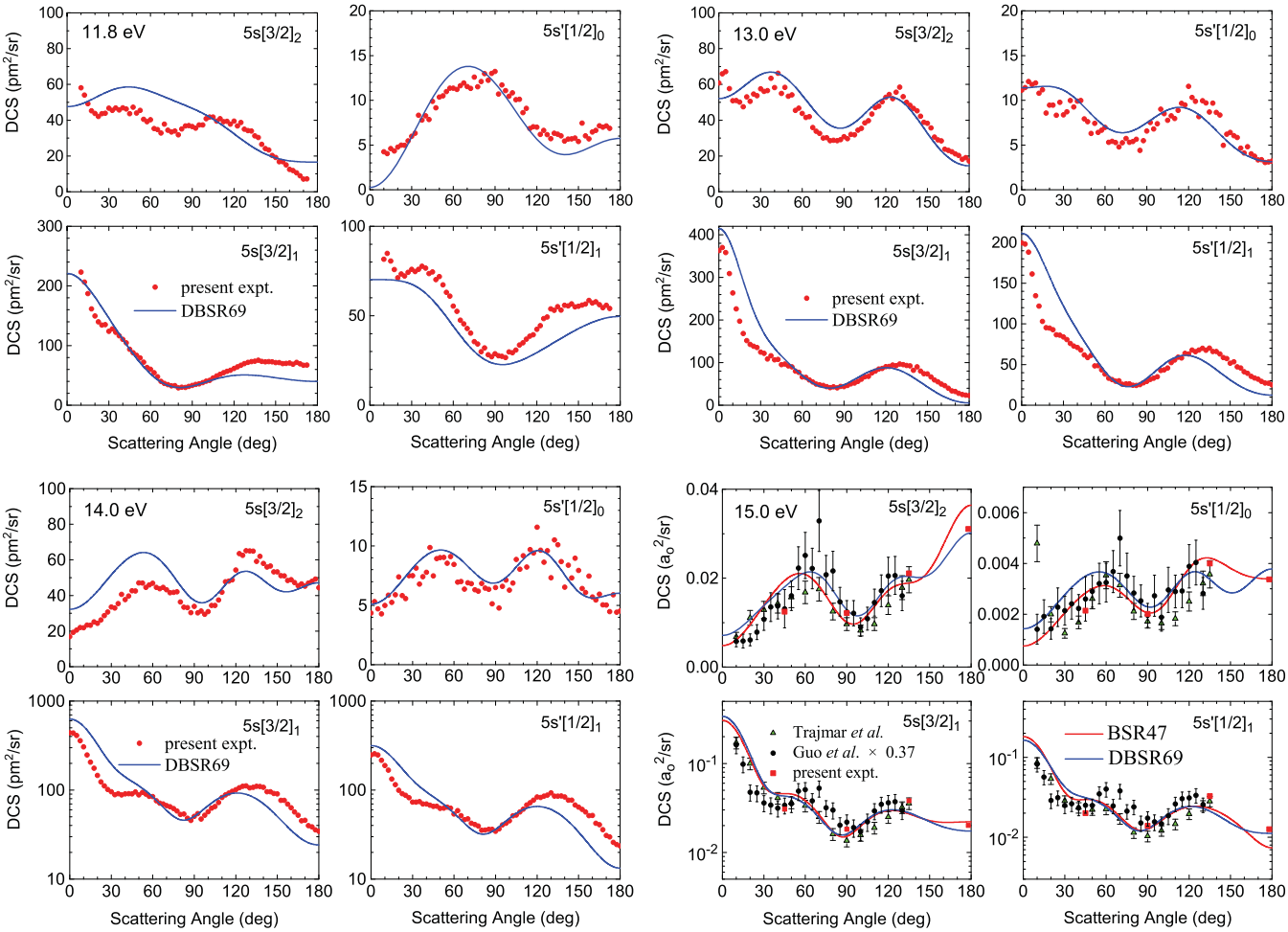

Figure 3. DCS for electron-impact excitation of the four states in the $4p^5$ 5s manifold of Kr at incident projectile energies of 11.8, 13.0, 14.0, and 15.0 eV. The experimental data are compared with theoretical predictions from the DBSR69 model and (for 15.0 eV only) the semi-relativistic BSR47 calculations. Also shown at 15.0 eV are the experimental data of Trajmar *et al* [15] and of Guo *et al* [16]. The latter were multiplied by 0.37 in order to fix a normalization error in the original publication [17].

Table 1. Angle-integrated cross sections (pm^2). We estimate the uncertainty in the experimental data to be about 20%.

State	$5s[3/2]_2$	$5s[3/2]_1$	$5s'[1/2]_0$	$5s'[1/2]_1$
$E = 11.8$ eV				
Experiment	458	832	114	613
DBSR69	523	837	125	586
BSR47	429	672	107	471
$E = 13$ eV				
Experiment	536	980	94	648
DBSR69	583	1052	99	688
BSR47	502	988	85	594
$E = 14$ eV				
Experiment	542	1060	95	789
DBSR69	601	1156	102	804
BSR47	544	1125	94	764

Angle-integrated cross sections derived from the experimental data of figure 3 are compared with the theoretical values in table 1. The experimental and both sets of theoretical results agree well within the experimental confidence limits of about 20%. The DBSR69 cross sections are on average about 6.5% higher and the BSR47 about 6.5% lower than experiment.

5. Conclusions

We have presented results from a detailed study of electron impact excitation of the $4p^5$ 5s states of Kr. Very satisfactory agreement between our absolute, high-resolution experimental data and predictions from a fully relativistic DBSR69 model was obtained, resolving likely normalization problems in previous experimental work. The experimental angular distributions extending over the entire angular range were used to derive assumption-free integral cross sections. They agree well with the predictions from both theoretical models. The success of the DBSR69 model gives us confidence in applying it to the even more complicated problem of e–Xe collisions and to compare the results with experimental benchmark data. A joint project for this system is currently in progress.

Acknowledgments

We thank Dr M A Khakoo for investigating the suspected problem with the data published in [16]. This work was supported by the Swiss National Science Foundation (project no 200020-131962) and the United States National Science Foundation under grants nos PHY-0757755 and PHY-0903818, as well as the TeraGrid allocation no TG-PHY090031.

References

[1] Buckman S J and Clark C W 1994 *Rev. Mod. Phys.* **66** 539
[2] Hoffmann T H, Ruf M-W, Hotop H, Zatsarinny O, Bartschat K and Allan M 2010 *J. Phys. B: At. Mol. Opt. Phys.* **43** 085206
[3] Phillips J M 1982 *J. Phys. B: At. Mol. Phys.* **15** 4259
[4] Zatsarinny O and Bartschat K 2004 *J. Phys. B: At. Mol. Opt. Phys.* **37** 2173
[5] Zatsarinny O 2006 *Comput. Phys. Commun.* **174** 273
[6] Zatsarinny O and Bartschat K 2008 *Phys. Rev.* A **77** 062701
[7] Allan M 1992 *J. Phys. B: At. Mol. Opt. Phys.* **25** 1559
[8] Nickel J C, Zetner P W, Shen G and Trajmar S 1989 *J. Phys. E: Sci. Instrum.* **22** 730
[9] Allan M 2000 *J. Phys. B: At. Mol. Opt. Phys.* **33** L215
[10] Allan M 2005 *J. Phys. B: At. Mol. Opt. Phys.* **38** 3655
[11] Allan M 2007 *J. Phys. B: At. Mol. Opt. Phys.* **40** 3531
[12] Noble C J 2008 private communication
[13] Burke V M and Noble C J 1995 *Comput. Phys. Commun.* **85** 471
[14] Grum-Grzhimailo A N 2003 *Comput. Phys. Commun.* **152** 101
[15] Trajmar S, Srivastava S K, Tanaka H, Nishimura H and Cartwright D C 1981 *Phys. Rev.* A **23** 2167
[16] Guo X *et al* 2000 *J. Phys. B: At. Mol. Opt. Phys.* **33** 1895
[17] Khakoo M A 2010 private communication